

Spin-wave excitations in the SDW state of iron pnictides: a comparison between the roles of interaction parameters

Dheeraj Kumar Singh*

Harish-Chandra Research Institute, Chhatnag Road, Jhansi, Allahabad 211019, India and
Homi Bhabha National Institute, Training School Complex, Anushakti Nagar, Mumbai 400085, India

We investigate the role of Hund's coupling in the spin-wave excitations of the $(\pi, 0)$ ordered magnetic state within a five-orbital tight-binding model for iron pnictides. To differentiate between the roles of intraorbital Coulomb interaction and Hund's coupling, we focus on the self-consistently obtained mean-field SDW state with a fixed magnetic moment obtained by using different sets of interaction parameters. We find that the Hund's coupling is crucial for the description of various experimentally observed characteristics of the spin-wave excitations including the anisotropy, energy-dependent behavior, and spin-wave spectral weight distribution.

PACS numbers: 74.70.Xa, 75.30.Ds, 75.30.Fv

I. INTRODUCTION

Iron-based superconductors are prototypes of moderately correlated^{1,2} and multiorbital systems exhibiting unconventional superconductivity (SC).³ A close proximity of the superconducting phase to the antiferromagnetic (AFM) phase^{4,5} indicates a crucial role of the spin fluctuations like in the cuprate superconductors. The pairing mediated by the spin-fluctuations has been a subject of intense investigation both theoretically and experimentally.^{6,7} An experimental signature of the role of spin-fluctuations, for instance, can be obtained in the form of change in magnetic-exchange energy involved in the transition from the normal to the superconducting state, which can then be compared with the superconducting condensation energy. The magnetic-exchange energy, on the other hand, can be estimated from the measurements of the spin excitations that yields information regarding the exchange coupling present in the system.^{8,9} Therefore, it is of much importance to comprehend various characteristics of the spin excitations for gaining insight into the mechanism of the Cooper pair formation.

Parent compounds of iron pnictides exhibit a spin-density wave state with ordering wavevector $\mathbf{Q} = (\pi, 0)$, which involves parallel ferromagnetic chains running along y direction while being coupled to each other antiferromagnetically along x .¹⁰ This particular spin arrangement arises due to the significant nesting present between the circular hole pockets at Γ and the elliptical electron pockets at X in the Fermi surfaces (FSs) of the unfolded Brillouin zone corresponding to one Fe atom per unit cell.¹¹⁻¹⁸ Existence of the Fermi surfaces in the SDW state,^{14,16} metallicity^{19,20} and small magnetic moments^{21,22} with largest being $\approx 1\mu_B$ found in 122 series supports the nesting based scenario. However, experimental investigation carried out by the inelastic neutron scattering (INS) measurements reveals remarkably high-energy scale of the spin-wave excitations, which are sharp, highly dispersive, and can extend up to energy ~ 200 meV.²³⁻²⁷

The spin-wave dispersion can be described within conventional Heisenberg model with highly anisotropic exchange couplings.²⁸ However, such a description suffers from the limitation that it cannot explain the spin-wave damping resulting from the particle-hole excitations in the metallic SDW state.

The limitation may be overcome by considering additional terms which account for the bandstructure and coupling between the electron spin and the local spin through Hund's coupling.²⁹ Various studies give an estimate of the intraorbital Coulomb interaction (U) to be $U/W \approx 0.25$, where W is the bandwidth.^{2,30} Therefore, plausibly a completely itinerant approach is best suited to describe the spin excitations in these materials. Within the latter approach, excitonic³¹ and orbital^{32,33} models have been frequently employed to investigate the spin-wave excitations. A comparative analysis of these two models while considering a two-orbital model has also been carried out, where excitations were found to be heavily damped away from the ordering wavevector \mathbf{Q} in the latter.³³

Standard on site interaction includes two important parameters - intraorbital Coulomb interaction U and Hund's coupling J . The correlation effect due to U involves the suppression of charge fluctuations whereas that due to J pertains to the unscreened high-spin state on the neighboring sites resulting in the correlations. Different values of U/J have often been used by different groups based on the different estimates from different methods. For instance, a combination of the constrained random-phase approximation and the maximally localized Wannier function yields $J/U \sim 0.14$ ³⁴ whereas work based on the dynamical mean-field theory estimates is $J/U \sim 0.25$.³⁵ Similarly, experiments also provide varying estimates for the same.^{2,36} With regard to various properties of this material, a comparative role of these two interaction parameters is of strong current interest.

U vs J phase diagrams in this direction is an important step.³⁷ Furthermore, in the two-orbital model, it has been illustrated that J plays an important role in stabilizing the doped SDW state against long-wavelength fluctuations through the generation of additional ferromagnetic spin coupling involving the inter-orbital susceptibility.³² The spin excitations have been studied recently within the five-orbital model as function of U but with a fixed Hund's coupling J .^{38,39} Well-defined branches extending upto high energy were obtained for those values of U that led to the magnetic moment $m \sim 1$ or larger. An important issue that has not attracted much attention is the role of J in the various features of spin-wave excitations such as dispersion, anisotropy and

the way spin-wave spectral weight is distributed.

In this paper, we examine the role of Hund's coupling in the spin-wave excitations of $(\pi, 0)$ SDW state of undoped iron pnictides within a five-orbital tight-binding model. The interaction parameters are chosen in such a way that a fixed magnetic moment $m \approx 1$ results in the self-consistent SDW state, which is motivated by the observed magnetic moments in 122 compounds. we find that J is crucial for (i) the sharp and well-defined excitations up to high energy, (ii) the anisotropy in the excitations around X, and (iii) the fact that the spin-wave spectral weight is concentrated near ~ 200 meV.

The plan of the paper is as follows. In section II, a mean-field description of the $(\pi, 0)$ SDW as well as the strategy to calculate spin-wave excitations is presented. In section III, results on the spin-wave dispersion along high-symmetry direction for different combination of intraorbital Coulomb interaction and Hund's coupling are presented. The way spin-wave spectral function behaves as a function of the interaction parameters is also discussed. Finally, conclusions are presented in section IV.

II. THEORY

The kinetic part of the model Hamiltonian that we consider is

$$\mathcal{H}_0 = \sum_{\mathbf{k}} \sum_{\mu, \nu} \sum_{\sigma} \varepsilon_{\mathbf{k}}^{\mu\nu} d_{\mathbf{k}\mu\sigma}^{\dagger} d_{\mathbf{k}\nu\sigma} + \text{H.c.}, \quad (1)$$

where the operator $d_{\mathbf{k}\mu\sigma}^{\dagger}$ ($d_{\mathbf{k}\mu\sigma}$) creates (destroys) an electron in the μ -th orbital with spin σ and momentum \mathbf{k} , and $\varepsilon_{\mathbf{k}}^{\mu\nu}$ are the hopping elements⁴⁰ from orbital μ to ν . The orbitals μ and ν belong to the set of five d -orbitals d_{xz} , d_{yz} , d_{xy} , $d_{x^2-y^2}$, and $d_{3z^2-r^2}$.

Standard onsite Coulomb interactions in the Hamiltonian

$$\begin{aligned} \mathcal{H}_{int} = & U \sum_{\mathbf{i}, \mu} n_{\mathbf{i}\mu\uparrow} n_{\mathbf{i}\mu\downarrow} + (U' - \frac{J}{2}) \sum_{\mathbf{i}, \mu < \nu} n_{\mathbf{i}\mu} n_{\mathbf{i}\nu} \\ & - 2J \sum_{\mathbf{i}, \mu < \nu} \mathbf{S}_{\mathbf{i}\mu} \cdot \mathbf{S}_{\mathbf{i}\nu} + J \sum_{\mathbf{i}, \mu < \nu, \sigma} d_{\mathbf{i}\mu\sigma}^{\dagger} d_{\mathbf{i}\mu\bar{\sigma}}^{\dagger} d_{\mathbf{i}\nu\bar{\sigma}} d_{\mathbf{i}\nu\sigma} \end{aligned} \quad (2)$$

include the intraorbital (interorbital) Coulomb interaction term as the first (second) term. The last two terms represent the Hunds coupling and the pair hopping energy, respectively.

The Hamiltonian in the $(\pi, 0)$ SDW state after mean-field approximation is obtained as

$$\mathcal{H}_{\mathbf{k}} = \sum_{\mathbf{k}\sigma} \Psi_{\mathbf{k}\sigma}^{\dagger} \begin{pmatrix} \hat{\varepsilon}_{\mathbf{k}} + \hat{N} & \text{sgn}\bar{\sigma}\hat{\Delta} \\ \text{sgn}\bar{\sigma}\hat{\Delta} & \hat{\varepsilon}_{\mathbf{k}+\mathbf{Q}} + \hat{N} \end{pmatrix} \Psi_{\mathbf{k}\sigma}, \quad (3)$$

where $\Psi_{\mathbf{k}\sigma}^{\dagger} = (c_{\mathbf{k}1\sigma}^{\dagger}, \dots, c_{\mathbf{k}5\sigma}^{\dagger}, c_{\mathbf{k}\bar{1}\sigma}^{\dagger}, \dots, c_{\mathbf{k}\bar{5}\sigma}^{\dagger})$ with $\bar{c}_{\mathbf{k}\bar{\mu}\sigma}^{\dagger} = c_{\mathbf{k}+\mathbf{Q}\mu\sigma}^{\dagger}$. Matrix elements of matrices \hat{M} and \hat{N} are

$$\begin{aligned} 2\Delta_{\mu\mu} &= U m_{\mu\mu} + J \sum_{\mu \neq \nu} m_{\nu\nu} \\ 2\Delta_{\mu\nu} &= J m_{\mu\nu} + (U - 2J) m_{\nu\mu} \end{aligned} \quad (4)$$

and

$$\begin{aligned} 2N_{\mu\mu} &= U n_{\mu\mu} + (2U - 5J) \sum_{\mu \neq \nu} n_{\nu\nu} \\ 2N_{\mu\nu} &= J n_{\mu\nu} + (4J - U) n_{\nu\mu}, \end{aligned} \quad (5)$$

where

$$n_{\mu\nu} = \sum_{\mathbf{k}\sigma} \langle c_{\mathbf{k}\mu\sigma}^{\dagger} c_{\mathbf{k}\nu\sigma} \rangle, \quad m_{\mu\nu} = \sum_{\mathbf{k}\sigma} \langle c_{\mathbf{k}\bar{\mu}\sigma}^{\dagger} c_{\mathbf{k}\nu\sigma} \rangle. \quad (6)$$

Multiorbital transverse-spin susceptibility is defined as

$$\begin{aligned} \chi_{\alpha\beta, \mu\nu}(\mathbf{q}, \mathbf{q}', i\omega_n) \\ = \frac{1}{\beta} \int_0^{\beta} d\tau e^{i\omega_n \tau} \langle T_{\tau} [S_{\alpha\beta}^+(\mathbf{q}, \tau) S_{\nu\mu}^-(\mathbf{q}', 0)] \rangle. \end{aligned} \quad (7)$$

Thus,

$$\begin{aligned} \chi_{\alpha\beta, \mu\nu}(\mathbf{q}, \mathbf{q}, i\omega_n) \\ = \sum_{\mathbf{k}, i\omega'_n} G_{\alpha\mu}^{0\uparrow}(\mathbf{k} + \mathbf{q}, i\omega'_n + i\omega_n) G_{\nu\beta}^{0\downarrow}(\mathbf{k}, i\omega'_n). \end{aligned} \quad (8)$$

The components of the spin operator in Eq. 7 are given by

$$\mathcal{S}_{\mathbf{q}}^i = \sum_{\mathbf{k}} \sum_{\sigma\sigma'} \sum_{\mu\mu'} d_{\mu\sigma}^{\dagger}(\mathbf{k} + \mathbf{q}) E_{\mu\mu'} \sigma_{\sigma\sigma'}^i d_{\mu'\sigma'}(\mathbf{k}), \quad (9)$$

where $i = x, y, z$, \hat{E} is a 5×5 identity matrix corresponding to the orbital bases, and σ^i are the Pauli matrices for the spin degree of freedom.

An element of the transverse-spin susceptibility in the SDW state is

$$\chi_{\alpha\beta, \mu\nu}^0 = \chi_{\alpha\beta, \mu\nu} + \chi_{\bar{\alpha}\bar{\beta}, \bar{\mu}\bar{\nu}} + \chi_{\alpha\bar{\beta}, \mu\bar{\nu}} + \chi_{\bar{\alpha}\bar{\beta}, \bar{\mu}\bar{\nu}}, \quad (10)$$

Then, the susceptibility matrix can be written as

$$\hat{\chi}^0(\mathbf{q}, i\omega_n) = \begin{pmatrix} \hat{\chi}^0(\mathbf{q}, \mathbf{q}, i\omega_n) & \hat{\chi}^0(\mathbf{q}, \mathbf{q} + \mathbf{Q}, i\omega_n) \\ \hat{\chi}^0(\mathbf{q} + \mathbf{Q}, \mathbf{q}, i\omega_n) & \hat{\chi}^0(\mathbf{q} + \mathbf{Q}, \mathbf{q} + \mathbf{Q}, i\omega_n) \end{pmatrix}, \quad (11)$$

where $\hat{\chi}^0(\mathbf{q}, \mathbf{q}, i\omega_n)$ and others are $n^2 \times n^2$ matrices. Physical transverse-spin susceptibility corresponding to the spin operators defined by Eq. 8 is

$$\chi^{ps}(\mathbf{q}, i\omega_n) = \sum_{\alpha\mu} \chi_{\alpha\alpha, \mu\mu}^0(\mathbf{q}, \mathbf{q}, i\omega_n). \quad (12)$$

Interaction effects are incorporated within the random-phase approximation (RPA) so that the spin susceptibility is given by

$$\hat{\chi}_{\text{RPA}}(\mathbf{q}, i\omega_n) = (\hat{\mathbf{1}} - \hat{U} \hat{\chi}^0(\mathbf{q}, i\omega_n))^{-1} \hat{\chi}^0(\mathbf{q}, i\omega_n). \quad (13)$$

Here, $\hat{\mathbf{1}}$ is a $2n^2 \times 2n^2$ identity matrix and the elements of block diagonal matrix \hat{U} are

$$\begin{aligned} & U_{\mu_1\mu_2; \mu_3\mu_4} \\ & = \begin{cases} U & (\mu_1 = \mu_2 = \mu_3 = \mu_4) \\ U - 2J & (\mu_1 = \mu_2 \neq \mu_3 = \mu_4) \\ J & (\mu_1 = \mu_2 \neq \mu_3 = \mu_4) \\ J & (\mu_1 = \mu_4 \neq \mu_2 = \mu_3) \\ 0 & (\text{otherwise}) \end{cases}, \end{aligned} \quad (14)$$

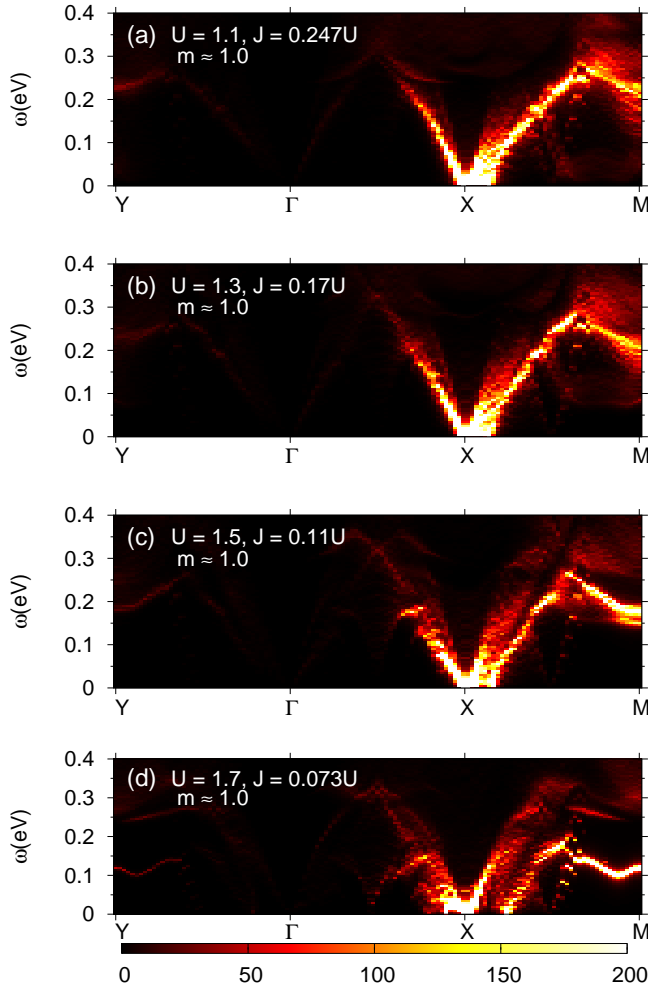


FIG. 1. Imaginary part of the RPA-level physical spin susceptibility $\text{Im}\chi_{\text{RPA}}^{ps}(\mathbf{q}, \omega)$ along the high-symmetry directions for the set of interaction parameters chosen in such a way that $m = 1$ in each case. (a) $U = 1.1, J = 0.247U$ (b) $U = 1.3, J = 0.167U$ (c) $U = 1.5, J = 0.110U$, and $U = 1.7$, and $J = 0.730U$.

where $U' = U - 2J$ has been used as required by the rotational invariance. Analytic continuation $i\omega_n \rightarrow \omega + i\eta$ in all the calculations described below is performed with η as 0.002eV. The unit of energy eV is used throughout unless stated otherwise.

III. RESULTS

Fig. 1 shows the imaginary part of RPA susceptibility $\text{Im}\chi_{\text{RPA}}^{ps}(\mathbf{q}, \omega)$ along the high-symmetry directions Y- Γ -X-M calculated in SDW state for values of U starting from 1.1 and increasing in step of 0.2 while J is chosen so that magnetic moment $m = 1$ with a maximum deviation only upto $\approx 2\%$. We find a strong dependence of several features of the self-consistent mean-field state on J as seen from the Table I, where the difference in the orbital-resolved magnetizations for the two set of parameters $U = 1.1, J = 0.247U$

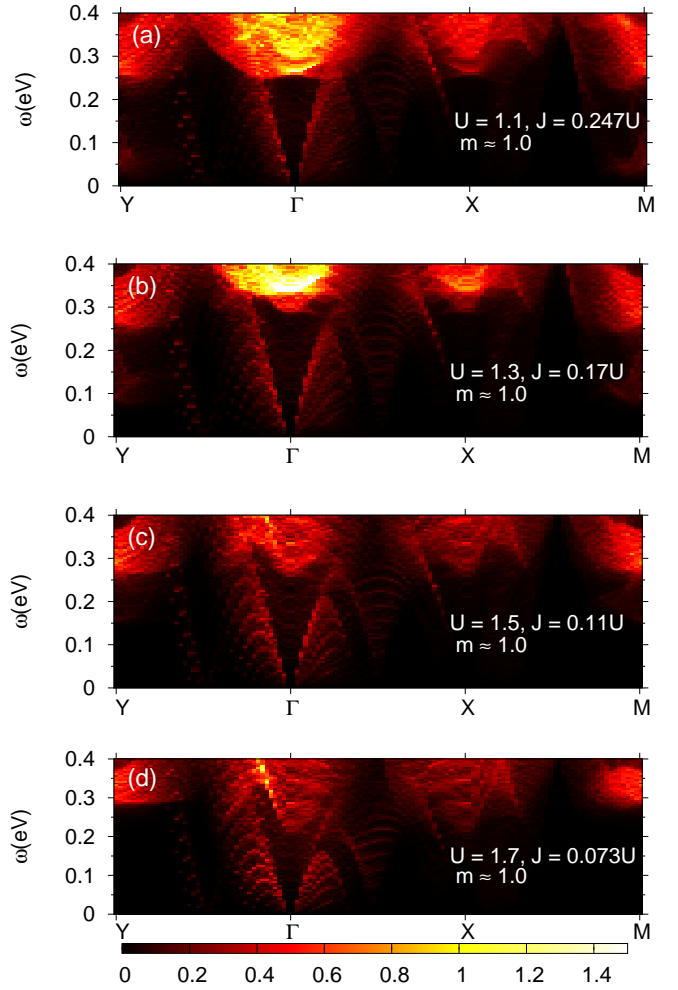


FIG. 2. Imaginary part of the bare physical spin susceptibility $\text{Im}\chi^{ps}(\mathbf{q}, \omega)$ along the high-symmetry directions for the set of interaction parameters as in Fig. 1.

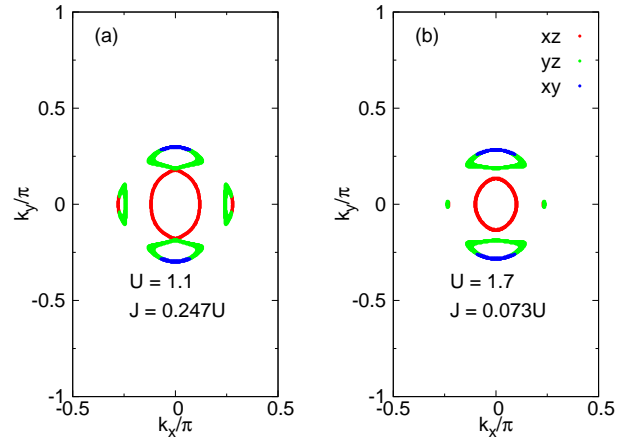


FIG. 3. FSs obtained for the two sets of interaction parameters (a) $U = 1.1, J = 0.247U$ and (b) $U = 1.7, J = 0.073U$. Magnetic moment $m = 1$ in each case. In both the cases, FSs include several pockets near Γ with a difference in the sizes.

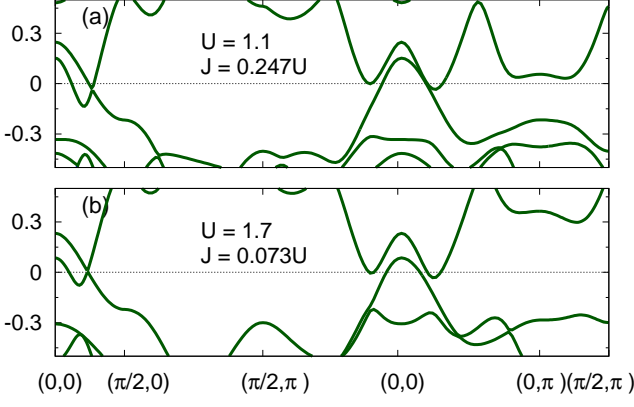


FIG. 4. Electron dispersions for (a) $U = 1.1, J = 0.247U$ and (b) $U = 1.7, J = 0.073U$ in the high-symmetry directions. Magnetic moment $m = 1$ in each case.

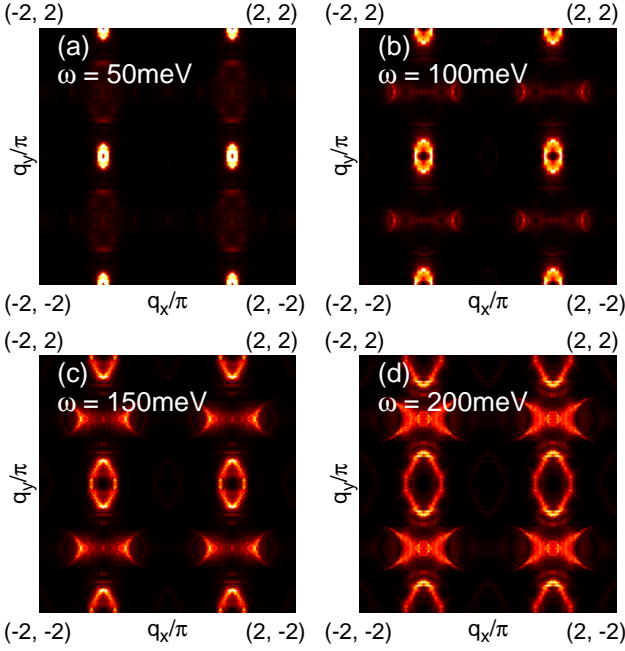


FIG. 5. Constant energy cuts of $\text{Im}\chi_{\text{RPA}}^{ps}(\mathbf{q}, \omega)$ for $U = 1.1, J = 0.247U$ at energies (a) 50 meV, (b) 100 meV, (c) 150 meV, and (d) 200 meV.

and $U = 1.7, J = 0.073U$ can be as large as $\approx 50\%$ (for $d_{3x^2-r^2}$ orbital) despite the same magnetic moment. A significant difference in the two cases can be noticed for all the orbitals except $d_{x^2-y^2}$. Further, orbital-resolved magnetization decreases for d_{xz} and d_{xy} and increases for the remaining orbitals, when J decreases.

Well-defined spin-wave excitations are obtained along Γ -X and in a part of X-M, where they can extend up to $\approx 0.2\text{eV}$ for $U = 1.1, J = 0.247U$ as shown in the Fig. 1(a). Contributions to the excitations are mainly from the intraorbital susceptibilities particularly corresponding to the orbitals d_{yz}, d_{yz} and d_{xy} with latter contributing the most as seen from the Table II and Table III. Tables show integrated spectral weight

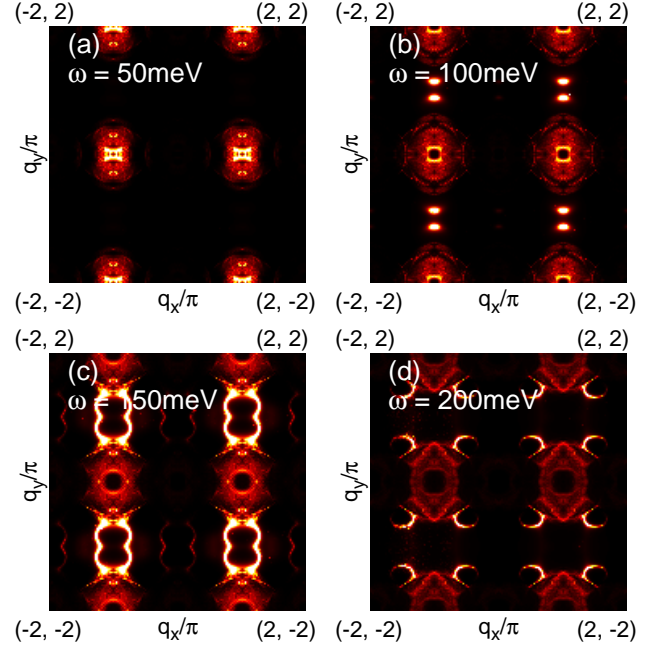


FIG. 6. Constant energy cuts of $\text{Im}\chi_{\text{RPA}}^{ps}(\mathbf{q}, \omega)$ for $U = 1.7, J = 0.073U$ at energies (a) 50 meV, (b) 100 meV, (c) 150 meV, and (d) 200 meV.

TABLE I. Orbital resolved magnetic moments and charge densities for the two cases $U = 1.1, J = 0.247U$ and $U = 1.7, J = 0.073U$ denoted by subscripts 1 and 2, respectively.

	$d_{3x^2-r^2}$	d_{xz}	d_{yz}	d_{xy}	$d_{x^2-y^2}$
n_1	1.457	1.230	1.165	0.982	1.165
n_2	1.574	1.309	1.189	0.834	1.094
m_1	0.160	0.155	0.252	0.338	0.098
m_2	0.099	0.185	0.197	0.422	0.075

$\sum_{\mathbf{q}, \omega} \text{Im}\chi_{\text{RPA}}^{ps}(\mathbf{q}, \omega)$ with the upper cutoff for the summation over ω chosen as $\omega_u = 0.5\text{eV}$. When J is decreased, contributions due to the interorbital susceptibilities also decrease whereas the contribution from the intraorbital susceptibility corresponding to d_{yz} orbital increases and becomes similar in magnitude to that corresponding to d_{xy} .

The excitations become increasingly broad and diffusive when J is small. However, exactly opposite happens near M, where they become rather sharp and non-diffusive. At the same time, energy of the spin-wave excitations near M increases. Heavy damping is present due to the metallicity of the SDW state as also reflected in the imaginary part of bare spin susceptibilities which appear gapless near Γ but are gapped in other regions (Fig. 2). The gap decreases in most part of the high-symmetry directions on decreasing J except near M, where it increases on the contrary. Ungapped imaginary part of the bare susceptibility derives from the fact that FSs exist for all the sets of parameters considered with the Fermi pockets being clustered around Γ (Fig. 3).

Behavior of the spin-excitations near M for smaller J indicate sharpness may not be always plausible particularly in the multiorbital systems like pnictides, where many bands are

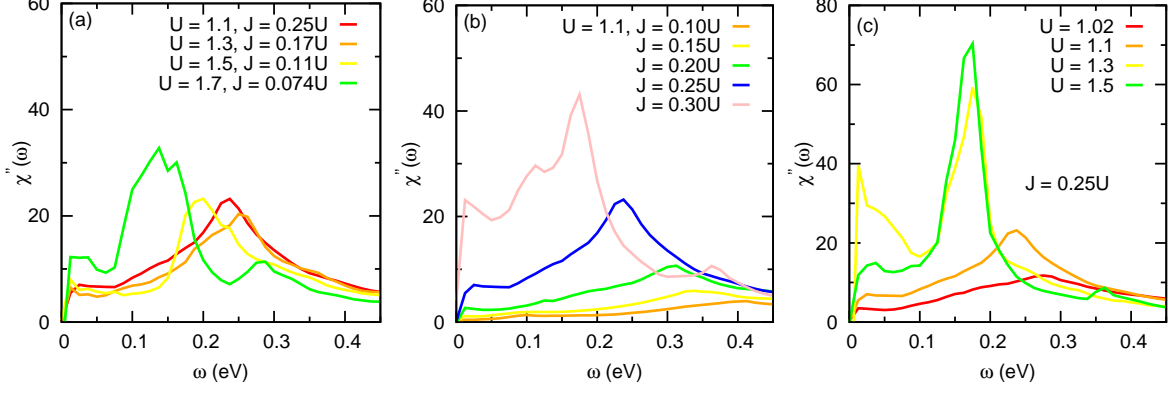


FIG. 7. Spin-wave spectral functions for the cases when (a) magnetic moment $m = 1$ whereas U and J are set constant in (b) and (c), respectively.

TABLE II. $\sum_{\mathbf{q},\omega} \text{Im} \chi_{\alpha\alpha,\beta\beta}^{sp}(\mathbf{q},\omega)$ at RPA-level for $U = 1.1$, $J = 0.247U$.

α/β	$d_{3x^2-r^2}$	d_{xz}	d_{yz}	d_{xy}	$d_{x^2-y^2}$
$d_{3x^2-r^2}$	0.030	0.023	0.030	0.039	0.019
d_{xz}	0.023	0.076	0.033	0.028	0.026
d_{yz}	0.030	0.033	0.101	0.032	0.032
d_{xy}	0.039	0.028	0.032	0.170	0.036
$d_{x^2-y^2}$	0.019	0.026	0.032	0.036	0.026

TABLE III. Same as in Table II but for $U = 1.7$, $J = 0.073U$.

α/β	$d_{3x^2-r^2}$	d_{xz}	d_{yz}	d_{xy}	$d_{x^2-y^2}$
$d_{3x^2-r^2}$	0.010	0.011	0.031	0.017	0.009
d_{xz}	0.011	0.085	0.021	0.003	0.019
d_{yz}	0.031	0.021	0.240	0.000	0.050
d_{xy}	0.017	0.003	0.000	0.250	0.027
$d_{x^2-y^2}$	0.009	0.019	0.050	0.027	0.040

located near the Fermi level. In order to understand the broadening especially near M when J is large, it is useful to examine the reconstructed bands in the SDW state, wherefrom it can be seen that a part of the lowest lying partially-filled band gets lowered further near $(0, \pi)$ on increasing J . Finally, it is in the immediate vicinity of the Fermi level for $U = 1.7$, $J = 0.073U$ as shown in Fig. 4 and may affect the imaginary part of the bare and RPA-level susceptibilities significantly, which are ungapped and heavily damped, respectively. At the same time, other portions of the bands remain largely unaffected. Thus, the unusual feature of spin-wave excitations near M may arise due to a subtle interplay between the roles of interaction and the bandstructure.

Fig. 5 and 6 show the energy cuts for $U = 1.1$, $J = 0.247U$ and $U = 1.7$, $J = 0.073U$, respectively. For the former case, anisotropy in the form of elliptical structure of excitations around X can be seen upto a energy as high as 200meV, where the major axis is oriented along Γ -Y. Excitations around M are rather broad and less intense with nature of anisotropy being similar to that around X. That changes quickly near 100meV

when the structure around M becomes extended along Γ -X. In contrast, anisotropy around X is relatively weak for the latter set of interaction parameters and is strong only in a narrow energy window around $\omega = 150\text{meV}$ for M. Moreover, the elliptical structure around X is also absent. Thus, anisotropy near Q particularly in the elliptical form is very sensitive to J . In both cases, the anisotropy continues to exist upto high energy. As revealed also by the INS measurements, a significant anisotropy with elliptical shape is present in the spin-wave excitations around X.^{10,24}

Fig. 7 shows the spin-wave spectral functions calculated for three different cases. When the magnetic moment $m \approx 1$ and a suitable set of interaction parameters is chosen, there is noticeable shift in the spectral weight towards low-energy region upon increasing U (Fig. 7 (a)). The hump-like peak structure located near 250meV for $U = 1.1$, $J = 0.247U$, which is in agreement with the experiments,²⁵ relocates near 125meV $U = 1.7$, $J = 0.073U$. Another important factor that can be responsible for the spectral weight shifting towards low-energy region is doping of holes or electrons, which will be discussed elsewhere. On the other hand, transfer of the spectral weight towards lower energy is significant in other two cases where one of the two interaction parameters is increased while keeping the other constant.

IV. CONCLUSIONS

To conclude, we have investigated the role of Hund's coupling in the spin-wave excitations of the SDW state of undoped iron pnictides by using a realistic electronic structure within a five-orbital model. We find that the Hund's coupling at the higher end of the range of various theoretical and experimental estimates ($J \sim U/4$) is required for the sharp and well-defined spin-wave dispersion in most part of the high-symmetry directions for a given magnetization. Not only that a similar value of Hund's coupling is also crucial for the elliptical shape of the anisotropy around Q $(\pi, 0)$ in the spin-wave excitations as well as for the spectral weight to be concentrated near energy $\gtrsim 200\text{meV}$. Thus, our study highlights the essential role of Hund's coupling in describing the exper-

imentally observed features of spin-wave excitations in the SDW state of undoped iron pnictides.

V. ACKNOWLEDGEMENT

We acknowledge the use of HPC clusters at HRI.

- * dheerajsingh@hri.res.in
- ¹ M. M. Qazilbash, J. J. Hamlin, R. E. Baumbach, Lijun Zhang, D. J. Singh, M. B. Maple, and D. N. Basov, *Nat. Phys.* **5**, 647 (2009).
 - ² W. L. Yang, A. P. Sorini, C-C. Chen, B. Moritz, W.-S. Lee, F. Vernay, P. Olalde-Velasco, J. D. Denlinger, B. Delley, J.-H. Chu, J. G. Analytis, I. R. Fisher, Z. A. Ren, J. Yang, W. Lu, Z. X. Zhao, J. van den Brink, Z. Hussain, Z.-X. Shen, and T. P. Devereaux, *Phys. Rev. B* **80**, 014508 (2009).
 - ³ G. R. Stewart, *Rev. Mod. Phys.* **83**, 1589 (2011).
 - ⁴ S. Avci, O. Chmaissem, D. Y. Chung, S. Rosenkranz, E. A. Goremychkin, J. P. Castellan, I. S. Todorov, J. A. Schlueter, H. Claus, A. Daoud-Aladine, D. D. Khalyavin, M. G. Kanatzidis, and R. Osborn, *Phys. Rev. B* **85**, 184507 (2012).
 - ⁵ N. Hussey, *Nat. Phys.* **12**, 290 (2016).
 - ⁶ D. J. Scalapino, *Rev. Mod. Phys.* **84**, 1383 (2012).
 - ⁷ T. Dahm, V. Hinkov, S. V. Borisenko, A. A. Kordyuk, V. B. Zabolotnyy, J. Fink, B. Büchner, D. J. Scalapino, W. Hanke, B. Keimer, *Nat. Phys.* **5**, 217 (2009).
 - ⁸ K.-J. Zhou, Y.-B. Huang, C. Monney, X. Dai, V. N. Strocov, N.-L. Wang, Z.-G. Chen, C. Zhang, P. Dai, L. Patthey, J. van den Brink, H. Ding, and Thorsten Schmitt, *Nat. Comms.* **4**, 1470 (2013).
 - ⁹ M. Wang, C. Zhang, X. Lu, G. Tan, H. Luo, Y. Song, M. Wang, X. Zhang, E. A. Goremychkin, T. G. Perring, T. A. Maier, Z. Yin, K. Haule, G. Kotliar, and P. Dai, *Nat. Comms.* **4**, 2874 (2013).
 - ¹⁰ J. Zhao, Q. Huang, C. de la Cruz, S. Li, J. W. Lynn, Y. Chen, M. A. Green, G. F. Chen, G. Li, Z. Li, J. L. Luo, N. L. Wang, and P. Dai, *Nat. Mat.* **7**, 953 (2008).
 - ¹¹ I. I. Mazin, D. J. Singh, M. D. Johannes, and M. H. Du, *Phys. Rev. Lett.* **101**, 057003 (2008).
 - ¹² D. J. Singh, and M.-H. Du, *Phys. Rev. Lett.* **100**, 237003 (2008).
 - ¹³ K. Haule, J. H. Shim, and G. Kotliar, *Phys. Rev. Lett.* **100**, 226402 (2008).
 - ¹⁴ M. Yi, D. H. Lu, J. G. Analytis, J.-H. Chu, S.-K. Mo, R.-H. He, M. Hashimoto, R. G. Moore, I. I. Mazin, D. J. Singh, Z. Hussain, I. R. Fisher, and Z.-X. Shen, *Phys. Rev. B* **80**, 174510 (2009).
 - ¹⁵ T. Kondo, R. M. Fernandes, R. Khasanov, Chang Liu, A. D. Palczewski, Ni Ni, M. Shi, A. Bostwick, E. Rotenberg, J. Schmalian, S. L. Bud'ko, P. C. Canfield, and A. Kaminski, *Phys. Rev. B* **81**, 060507(R) (2010).
 - ¹⁶ M. Yi, D. Lu, J.-H. Chu, J. G. Analytis, A. P. Sorini, A. F. Kemper, B. Moritz, S.-K. Mo, R. G. Moore, M. Hashimoto, W.-S. Lee, Z. Hussain, T. P. Devereaux, I. R. Fisher, and Z.-X. Shen, *Proc. Nat. Acad. Science* **108**, 6878 (2011).
 - ¹⁷ V. Brouet, M. F. Jensen, P.-H. Lin, A. Taleb-Ibrahimi, P. Le Fèvre, F. Bertran, C.-H. Lin, Wei Ku, A. Forget, and D. Colson, *Phys. Rev. B* **86**, 075123 (2012).
 - ¹⁸ A. A. Kordyuk, V. B. Zabolotnyy, D. V. Evtushinsky, A. N. Yaresko, B. Büchner, and S. V. Borisenko, *J. Supercond. Nov. Magn.* **26**, 2837 (2013).
 - ¹⁹ T-M Chuang, M. P. Allan, J. Lee, Xie Yang, Ni Ni, S. L. Bud'ko, G. S. Boebinger, P. C. Canfield, and J. C. Davis, *Science* **327**, 181 (2010).
 - ²⁰ M. Nakajima, T. Liang, S. Ishida, Y. Tomioka, K. Kihou, C. H. Lee, A. Iyo, H. Eisaki, T. Kakeshita, T. Ito, and S. Uchida, *Proc. Natl. Acad. Sci. U.S.A.* **108**, 12238 (2011).
 - ²¹ C. de la Cruz, Q. Huang, J. Lynn, J. Li, W. Ii, J. Zarestky, H. Mook, G. Chen, J. Luo, N. Wang, and P. Dai, *Nature*, **453**, 899 (2008).
 - ²² Q. Huang, Y. Qiu, Wei Bao, M. A. Green, J. W. Lynn, Y. C. Gasparovic, T. Wu, G. Wu, and X. H. Chen, *Phys. Rev. Lett.* **101**, 257003 (2008).
 - ²³ R. A. Ewings, T. G. Perring, R. I. Bewley, T. Guidi, M. J. Pitcher, D. R. Parker, S. J. Clarke, and A. T. Boothroyd, *Phys. Rev. B* **78**, 220501(R) (2008).
 - ²⁴ S. O. Diallo, V. P. Antropov, T. G. Perring, C. Broholm, J. J. Pulkittil, N. Ni, S. L. Bud'ko, P. C. Canfield, A. Kreyssi, A. I. Goldman, and R. J. McQueeney, *Phys. Rev. Lett.* **102**, 187206 (2009).
 - ²⁵ J. Zhao, D. T. Adroja, Dao-Xin Yao, R. Bewley, S. Li, X. F. Wang, G. Wu, X. H. Chen, J. Hu, and P. Dai, *Nat. Phys.* **5**, 555 (2009).
 - ²⁶ L. W. Harriger, H. Q. Luo, M. S. Liu, C. Frost, J. P. Hu, M. R. Norman, and P. Dai, *Phys. Rev. B* **84**, 054544 (2011).
 - ²⁷ R. A. Ewings, T. G. Perring, J. Gillett, S. D. Das, S. E. Sebastian, A. E. Taylor, T. Guidi, and A. T. Boothroyd, *Phys. Rev. B* **83**, 214519 (2011).
 - ²⁸ D.-X. Yao and E. W. Carlson, *Phys. Rev. B* **78**, 052507 (2008).
 - ²⁹ W. Lv, F. Krüger, and P. Phillips, *Phys. Rev. B* **82**, 045125 (2010).
 - ³⁰ V. I. Anisimov, Dm. M. Korotin, M. A. Korotin, A. V. Kozhevnikov, J. Kuneš, A. O. Shorikov, S. L. Skornyakov, and S V Streltsov, *J. Phys.: Condens. Matter* **21**, 075602 (2009).
 - ³¹ P. M. R. Brydon and C. Timm, *Phys. Rev. B* **80**, 174401 (2009).
 - ³² N. Raghuvanshi and A. Singh, *J. Physics: Condens. Matter* **22**, 422202 (2010).
 - ³³ J. Knolle, I. Eremin, and R. Moessner, *Phys. Rev. B* **83**, 224503 (2011).
 - ³⁴ T. Miyake, K. Nakamura, R. Arita, and M. Imada, *J. Phys. Soc. Jpn.* **79**, 044705 (2010).
 - ³⁵ H. Ishida and A. Liebsch, *Phys. Rev. B* **81**, 054513 (2010).
 - ³⁶ A. A. Schafgans, S. J. Moon, B. C. Pursley, A. D. LaForge, M. M. Qazilbash, A. S. Sefat, D. Mandrus, K. Haule, G. Kotliar, and D. N. Basov, *Phys. Rev. Lett.* **108**, 147002 (2012).
 - ³⁷ Q. Luo, G. Martins, D.-X. Yao, M. Daghofer, R. Yu, A. Moreo, and E. Dagotto, *Phys. Rev. B* **82**, 104508 (2010).
 - ³⁸ E. Kaneshita, and T. Tohyama, *Phys. Rev. B* **82**, 094441 (2010).
 - ³⁹ M. Kovacic, M. H. Christensen, M. N. Gastiasoro, and B. M. Andersen, *Phys. Rev. B* **91**, 064424 (2015).
 - ⁴⁰ H. Ikeda, R. Arita, and J. Kunes, *Phys. Rev. B* **81**, 054502 (2010).